ISSN 1674-1056
http://cpb.iphy.ac.cn
http://iopscience.iop.org/cpb
中国物理 B
Chinese Physics
中国物理
Chinese Physics B

Simulation research on effect of magnetic nanoparticles on physical process of magneto-acoustic tomography with magnetic induction

Xiao-Heng Yan(闫孝姮), Ying Zhang(张莹), Guo-Qiang Liu(刘国强)

Citation: Chin. Phys. B . 2018, 27(10): 104302. **doi:** 10.1088/1674-1056/27/10/104302

Journal homepage: http://cpb.iphy.ac.cn; http://iopscience.iop.org/cpb

What follows is a list of articles you may be interested in

A local energy-preserving scheme for Zakharov system

Qi Hong(洪旗), Jia-ling Wang(汪佳玲), Yu-Shun Wang(王雨顺)

Chin. Phys. B . 2018, 27(2): 020202. **doi:** 10.1088/1674-1056/27/2/020202

Boundary normal pressure-based electrical conductivity reconstruction for magneto-acoustic tomography with magnetic induction

Ge-Pu Guo(郭各朴), He-Ping Ding(丁鹤平), Si-Jie Dai(戴思捷), Qing-Yu Ma(马青玉)

Chin. Phys. B . 2017, 26(8): 084301. **doi:** 10.1088/1674-1056/26/8/084301

Conductivity reconstruction algorithms and numerical simulations for magneto-acousto-electrical tomography with piston transducer in scan mode

Guo Liang, Liu Guo-Qiang, Xia Hui, Liu Yu, Lu Min-Hua

Chin. Phys. B . 2014, 23(10): 104303. **doi:** 10.1088/1674-1056/23/10/104303

Multifunctional magnetic nanoparticles for magnetic resonance image-guided photothermal therapy for cancer

Yue Xiu-Li, Ma Fang, Dai Zhi-Fei

Chin. Phys. B . 2014, 23(4): 044301. **doi:** 10.1088/1674-1056/23/4/044301

Magnetic microbubble：A biomedical platform co-constructed from magnetics and acoustics

Yang Fang, Gu Zhu-Xiao, Jin Xin, Wang Hao-Yao, Gu Ning

Chin. Phys. B . 2013, 22(10): 104301. **doi:** 10.1088/1674-1056/22/10/104301

Simulation research on effect of magnetic nanoparticles on physical process of magneto–acoustic tomography with magnetic induction*

Xiao-Heng Yan(闫孝姮)[1,2], Ying Zhang(张莹)[1,2], and Guo-Qiang Liu(刘国强)[2,3,†]

[1] *Faculty of Electrical and Control Engineering, Liaoning Technical University, Huludao* 125105, *China*
[2] *Institute of Electrical Engineering, Chinese Academy of Sciences, Beijing* 100190, *China*
[3] *School of Electronic Electrical and Communication Engineering, University of Chinese Academy of Sciences, Beijing* 101407, *China*

(Received 6 June 2018; revised manuscript received 13 August 2018; published online 27 September 2018)

Magneto–acoustic tomography with magnetic induction (MAT-MI) is a multiphysics coupled imaging technique that is combined with electrical impedance tomography and ultrasound imaging. In order to study the influence of adding magnetic nanoparticles as a contrast agent for MAT-MI on its physical process, firstly, we analyze and compare the electromagnetic and acoustical properties of MAT-MI theoretically before and after adding magnetic nanoparticles, and then construct a two-dimensional (2D) planar model. Under the guidance of space-time separation theory, we determine the reasonable simulation conditions and solve the electromagnetic field and sound field physical processes in the two modes by using the finite element method. The magnetic flux density, sound pressure distribution, and related one-dimensional (1D), 2D, and three-dimensional(3D) images are obtained. Finally, we make a qualitative and quantitative analysis based on the theoretical and simulation results. The research results show that the peak time of the time item separated from the sound source has a corresponding relationship with the peak time of the sound pressure signal. At this moment, MAMPT-MI produces larger sound pressure signals, and the sound pressure distribution of the MAMPT-MI is more uniform, which facilitates the detection and completion of sound source reconstruction. The research results may lay the foundation for the MAT-MI of magnetically responsive nanoparticle in subsequent experiments and even clinical applications.

Keywords: magneto–acoustic tomography with magnetic induction, magnetic nanoparticles, magnetic flux density, sound pressure

PACS: 43.35.Rw, 02.60.Cb, 43.20.Bi **DOI:** 10.1088/1674-1056/27/10/104302

1. Introduction

Magneto-acoustic tomography with magnetic induction (MAT-MI), a multi-physics coupled imaging method, has attracted much attention recently. The MAT-MI was first proposed by He Bin *et al.* in 2005 and has received extensive attention in recent years.[1] The research on MAT-MI aims to improve the resolution of imaging. The research mainly focuses on theoretical analysis,[2–4] simulations,[5] scanning systems,[6–8] reconstruction algorithms,[9–16] and biological tissue experiments.[17,18] In recent years, in order to enhance the imaging effect in imaging, magnetic nanoparticles have been used as contrast agents to set off research booms. It is combined with MAT-MI as a drug carrier for targeting, and the combination of drug therapy and imaging monitoring is a current research hotspot. In 2012, Hu *et al.* proposed to incorporate magnetic nanoparticles into the MAT-MI for the first time.[19] The tissue model containing superparamagnetic nanoparticles was examined and a clear tissue boundary image was obtained. It provided a new detection technology for the detection of magnetic nanomaterials in drug transport and targeted therapy, and it further proved that the MAT-MI has unique advantages in the fields of gene therapy and molecular imaging. In 2013, Carrey *et al.* described the excitation conditions of the magneto-acoustic signals of nanoparticles in an alternating magnetic field.[20] In the same year, Steinberg *et al.* proposed a method of detecting target objects based on nanoparticle magneto-acoustic signals, and used the magnetic acoustic signals generated by the nanoparticles in an alternating magnetic field to obtain information about the location of the target.[21] In 2014, Fang *et al.* conducted the research on magnetic sensing nano-sensing technology, established a magnetic induction magneto-acoustic nano-sensing experimental system, and conducted an experimental study on the uniform distribution of magnetic nanoparticles. The experiments proved that magnetic signals can be detected.[22] In 2016, Mariappan *et al.* embedded superparamagnetic iron oxide nanoparticles into mice and successfully detected and reconstructed the distribution of superparamagnetic iron oxide nanoparticles by using the MAT-MI. It proved that magnetic nanoparticle-based MAT-MI has good resolution and imaging depth and can be used for imaging the soft tissue tumors.[23]

However, most of the current researches focus on the detection of magneto-acoustic signals and the acquisition of tissue boundary images. There has been no report on the prin-

*Project supported by the National Natural Science Foundation of China (Grant Nos. 51507171,and 61427806).
†Corresponding author. E-mail: liuguoqiang@mail.iee.ac.cn
© 2018 Chinese Physical Society and IOP Publishing Ltd

ciple analysis of magneto-nanoparticles and their detailed introduction. In view of this, we carry out a research on the electromagnetic and acoustic fields of MAT-MI by using magnetic nano-particles. We establish a 2D planar model of the imaging target, analyze the effects of the introduction of magnetic nanoparticles on the distribution of magnetic flux density and the sound pressure distribution of the sound field from the theory and simulation, and compare the magnetic flux density and sound pressure signals before and after the introduction of nanoparticles. Finally we conduct a preliminary qualitative and quantitative analysis of the effects of magnetic nanoparticles on MAT-MI.

2. Theoretical analysis

2.1. Principle of tomography

As shown in Fig. 1, an alternating magnetic field $\tilde{\boldsymbol{B}}$ is applied to the object space, where $\tilde{\boldsymbol{B}}$ is generated by a z-direction alternating current $\tilde{\boldsymbol{J}}_0$ which is applied to a current-carrying conductor placed on the xz plane. The magnetic field is mainly along the x direction of the object space. The target body induces an eddy current $\tilde{\boldsymbol{J}}$ under the action of an alternating magnetic field. The eddy current interacts with a static magnetic field and an alternating magnetic field to generate a Lorentz force $\tilde{\boldsymbol{f}}$, and the target body vibrates to generate an acoustic wave.

At this time, the abnormal conductivity body exists as a sound source, and the essence of the imaging is to detect the abnormality of the conductivity. Therefore, in this paper, this imaging method is called magneto–acoustic impedance tomography with magnetic induction (MAIT-MI).

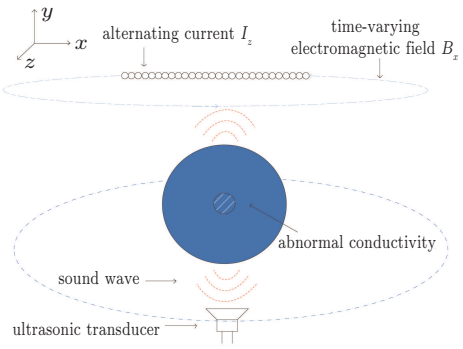


Fig. 1. (color online) Schematic diagram of MAIT-MI.

After the introduction of magnetic nanoparticles as shown in Fig. 2, the source of the force changes, and the Lorentz force changes into the electromagnetic force generated by the magnetic nanoparticles under the action of an alternating magnetic field. At this point, the sound source that causes the particle vibration to produce sound waves is a magnetic nanoparticle. The essence of imaging is to detect the abnormality of magnetic permeability. Therefore, in this paper, this imaging method is called magneto-acoustic magnetic permeability tomography with magnetic induction (MAMPT-MI).

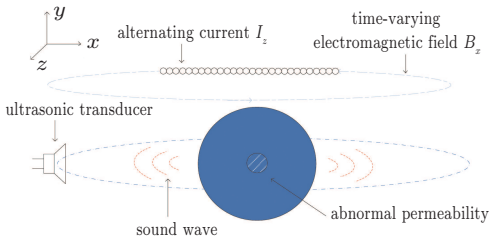


Fig. 2. (color online) Schematic diagram of MAMPT-MI.

2.2. Sound field characteristics

For a biological tissue medium that can be viewed as a non-viscous fluid, the acoustic field continuity equation[24] is

$$\frac{\partial(\rho+\rho_0)}{\partial t} = -\nabla\cdot(\rho\tilde{\boldsymbol{v}}+\rho_0\tilde{\boldsymbol{v}}). \tag{1}$$

The sound field motion equation is

$$(\rho+\rho_0)\left(\frac{\partial\tilde{\boldsymbol{v}}}{\partial t}+\tilde{\boldsymbol{v}}\cdot\nabla\tilde{\boldsymbol{v}}\right)+\nabla(p_0+p)-\tilde{\boldsymbol{f}}=0, \tag{2}$$

where ρ_0 denotes the medium density without disturbance, p_0 is the medium pressure without disturbance, ρ is sound-induced density disturbances, $\tilde{\boldsymbol{v}}$ is the vibration velocity of the particles in the medium, and p is the sound pressure.

After omitting higher order small quantities in the equation, the continuous equation and motion equation are obtained as follows:

$$\frac{\partial\rho}{\partial t} = -\rho_0\nabla\cdot\tilde{\boldsymbol{v}}, \tag{3}$$

$$\rho_0\frac{\partial\boldsymbol{v}}{\partial t} = -\nabla p+\tilde{\boldsymbol{f}}. \tag{4}$$

Meanwhile, the equation of state is

$$p = c_{\mathrm{s}}^2\rho. \tag{5}$$

Simultaneous equations (3)–(5) can be used to derive the coupling equation of sound pressure and particle velocity

$$\begin{cases}\dfrac{1}{c_{\mathrm{s}}^2}\dfrac{\partial p}{\partial t} = -\rho_0\nabla\cdot\tilde{\boldsymbol{v}},\\ \rho_0\dfrac{\partial\tilde{\boldsymbol{v}}}{\partial t} = \nabla p+\tilde{\boldsymbol{f}}.\end{cases} \tag{6}$$

In this way, the sound pressure wave equation can be derived

$$\frac{1}{\rho_0}\nabla^2-\frac{1}{\rho_0 c_{\mathrm{s}}^2}\frac{\partial^2 p}{\partial t^2} = \frac{1}{\rho_0}\nabla\cdot\tilde{\boldsymbol{f}}. \tag{7}$$

2.3. Sound source

According to the principle of MAIT-MI, the source term $\tilde{\boldsymbol{f}}$ in Eq. (7) is the Lorentz force. Assume that there is only a magnetic field in the x direction, then we will obtain

$$\tilde{\boldsymbol{f}} = \tilde{\boldsymbol{J}}\times\tilde{\boldsymbol{B}} = \tilde{J}_z\tilde{B}_x\tilde{\boldsymbol{e}}_y, \tag{8}$$

where $\tilde{J}_z$ is the induced current in the target body and $\tilde{B}_x$ is the magnetic field in the x direction.

For the MAMPT-MI, when magnetic nanoparticles are exposed to an external magnetic field, the magnetic energy of a single particle is[25]

$$U = \frac{1}{2}\tilde{\boldsymbol{m}} \cdot \tilde{\boldsymbol{B}} = -\frac{\chi_{\rm np} v_{\rm np} f_{\rm m}}{2\mu_0}\tilde{\boldsymbol{B}}^2, \tag{9}$$

where χ is the magnetic susceptibility of the particle, $v_{\rm np}$ is the volume of the nanoparticles, $f_{\rm m}$ is the volume fraction of the nanoparticles, and μ_0 is the permeability constant of the vacuum.

Then the electromagnetic force can be calculated according to the principle of virtual work, and expressed as

$$\tilde{\boldsymbol{f}} = -\frac{\chi_{\rm np} v_{\rm np} f_{\rm m}}{2\mu_0}\nabla\left|\tilde{\boldsymbol{B}}\right|^2. \tag{10}$$

Assuming that only the magnetic field in the x direction is considered, the sound source term in Eq. (7) is electromagnetic force and can be expressed as

$$\tilde{\boldsymbol{f}} = -\frac{\chi_{\rm np} v_{\rm np} f_{\rm m}}{\mu_0}\tilde{B}_x\frac{\partial \tilde{B}_x}{\partial x}\boldsymbol{e}_x. \tag{11}$$

2.4. Theoretical basis of time waveform analysis

The alternating current and its generated all physical quantities are time-varying vectors, and any time-varying vector can be expressed as the product of the space vector term and the time term. In this article, we call it the theory of space-time separation.

The magnetic quasi-static approximation is used to analyze the sound source time terms of MAIT-MI and MAMPT-MI. First, introduce the time term, record the alternating current as $\tilde{\boldsymbol{J}} = \boldsymbol{J}_0 s(t)$, and ignore the influence of the displacement current, then will have

$$\nabla \times \tilde{\boldsymbol{H}}_1 = \tilde{\boldsymbol{J}}_0. \tag{12}$$

It can be seen that the magnetic field strength and magnetic flux density of a primary magnetic field can be expressed as $\tilde{\boldsymbol{H}}_1 = \boldsymbol{H}_1 s(t)$ and $\tilde{\boldsymbol{B}} = \boldsymbol{B}_1 s(t)$, respectively.

For the MAIT-MI, the electrical anomaly is a low-conductivity biological tissue model, and the secondary magnetic field is much smaller than the primary magnetic field, so the effect of the secondary magnetic field can be ignored. Therefore

$$\nabla \times \tilde{\boldsymbol{E}} = -\frac{\partial \tilde{\boldsymbol{B}}}{\partial t} = -\boldsymbol{B}_1\frac{{\rm d}s}{{\rm d}t} = \boldsymbol{B}_1 g(t), \tag{13}$$

where $\tilde{\boldsymbol{E}}$ is the induced electric field strength, $g(t) = {\rm d}s/{\rm d}t$. Therefore, the induced electric field can be expressed as $\tilde{\boldsymbol{E}} = \boldsymbol{E}g(t)$.

According to Ohm's law $\tilde{\boldsymbol{J}} = \sigma\tilde{\boldsymbol{E}}$, the induced current in the abnormal conductivity body is $\tilde{\boldsymbol{J}} = \boldsymbol{J}g(t)$.

Therefore, it can be seen that the sound source item of MAIT-MI is

$$\tilde{\boldsymbol{f}} = \tilde{\boldsymbol{J}} \times \tilde{\boldsymbol{B}} = \left(\boldsymbol{J} \times \boldsymbol{B}\right)s(t)g(t). \tag{14}$$

For the MAMPT-MI, the sound source is only related to magnetic field and its gradient, so the sound source item can be written as

$$\tilde{\boldsymbol{f}} = -\frac{\chi_{\rm np} v_{\rm np} f_{\rm m}}{\mu_0}B_x\frac{\partial B_x}{\partial x}\boldsymbol{e}_x s^2(t). \tag{15}$$

3. Numerical simulation

In this paper, a multi-physics coupling software comsol multiphysics was used to establish a biological tissue simulation model and a finite element analysis of the electromagnetic field. The model is shown in Fig. 3.

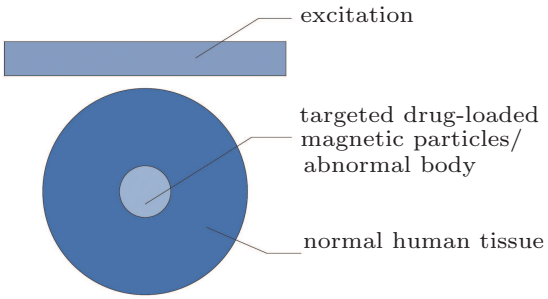


Fig. 3. (color online) The 2D plane simulation model.

Considering the concentric model, the center of the circle is set at the origin of the coordinates. The outer circle represents the normal tissue and its radius is 400 nm. Since the analysis of the general rule is not affected in this paper, the conductivity is set to be 0 S/m; the relative permittivity and relative permeability are both set to be 1; the inner circle is set to be the target drug-loaded magnetic particles or abnormal body according to different simulation conditions with a radius of 50 nm; the electromagnetic field background environment conductivity is defined as 0 S/m; the relative permittivity and relative permeability are both set to be 1. The parameter settings are shown in Table 1.

Table 1. Simulation parameters.

Variable	Parameter	Simulation value
μ	relative permeability of magnetic anomaly	6
σ	conductivity of electrical anomaly	5 S/m
$r_{\rm i}$	radius of outer circle	400 nm
$r_{\rm o}$	radius of inner circle	50 nm
σ_0	background environment conductivity	0 S/m

In order to save computer resources and speed up calculations, different grid sizes are set for the solution area to solve the finite element problem, and meshing is performed. Performing transient analysis to solve the electromagnetic field, the applied current density excitation pulse function is shown in Fig. 4 and its expression is as follows:

$$f(t) = 2 \times 10^8 \times \mathrm{e}^{-5\times 10^6 t} \times \sin\left(2\pi \times \times 10^6 t\right) \tag{16}$$

To avoid the edge effect, the current density excitation is set to be in the z direction, that is, the target body is placed in the x-direction magnetic field, and the applied current density is converted into a current amplitude of about 80 A. The parameters are matched with the magnetic acoustic imaging experimental platform.

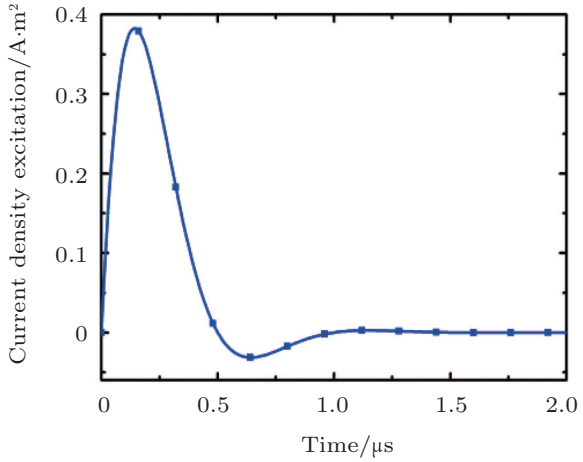


Fig. 4. (color online) Current density excitation.

The targeted drug-loaded magnetic nanoparticle used in this paper is shown in Fig. 5. It represents a magnetic drug-loaded particle cluster model with superparamagnetic nanoparticles with an average diameter of 3 nm–4 nm, embedded in a biocompatible polymer. The model has a nuclear structure, and the size of a single particle structure is still on a nano-scale. The diameter of the combined superparamagnetic nanoparticle stable clusters is usually in a range between 10 n, and 400 nm, and it is assumed to be a sphere for the simulation study of the magneto-acoustic physics process.[26]

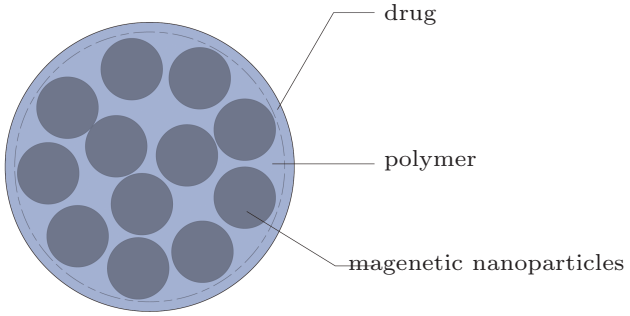


Fig. 5. (color online) Superparamagnetic nanoparticles stable cluster.

3.1. Time source curve of sound source

Through the analysis of the time waveform, it can be seen that the sound source time items of MAIT-MI and MAMPT-MI are

$$Q_{\mathrm{i}} = s(t)g(t) \tag{17}$$

$$Q_{\mathrm{m}} = s^2(t). \tag{18}$$

Then we can draw a one-dimensional (1D) curve of the time item as shown in Fig. 6. It can be seen that the time peaks of MAIT-MI and MAMPT-MI occur at 0.06 μs and 0.2 μs, respectively.

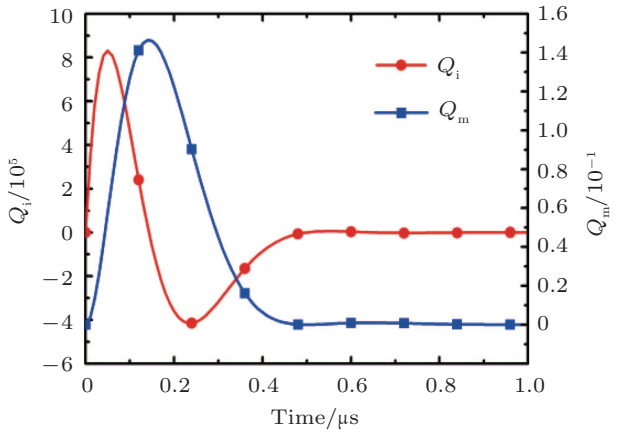


Fig. 6. (color online) The 1D curve of sound source time item of MAIT-MI (red line) and MAMPT-MI (blue line).

3.2. Effect of magnetic nanoparticles on magnetic flux density

In order to verify the enhancement effect of magnetic nanoparticles on the imaging effect, the MAIT-MI is used as a reference in this paper, and the simulation comparisons are made of both the magnetic flux density and sound pressure distribution in the imaging target body. The MAIT-MI is based on the principle of early changes in electrical characteristics of diseased tissue and the target of detection is the electrical conductivity of anomalous body. In Fig. 3, the inner circle of concentric circles is an electrical anomaly, and the conductivity is set to be $\sigma = 5$ S/m. The MAMPT-MI is a targeted combination of magnetic nanoparticles and diseased tissue. The detection target is magnetic permeability of magnetic nanoparticles. The inner circle of the concentric circle in the model is a magnetic anomaly, and the relative permeability is set to be $\mu = 6$. The simulation is conducted under the magnetic quasi-static condition, the electromagnetic field module and the sound field module are adopted, and equations (8) and (11) are used as a dipole source of the sound field for simulation analysis. The magnetic flux density distributions of the two imaging modes are calculated, and the results are shown in Fig. 7.

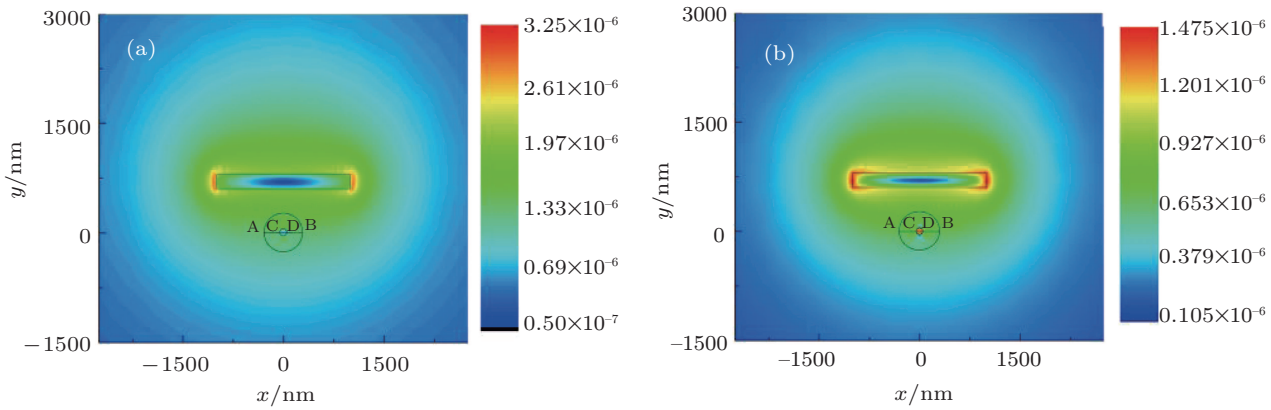


Fig. 7. (color online) Magnetic flux density distributions of two imaging methods, obtained according to peak time calculated by space-time separation method. (a) $t = 0.06$ μs, MAIT-MI flux density distribution; (b) $t = 0.2$ μs, MAMPT-MI flux density distribution.

The two models are in the same time-varying magnetic field, while the effects of the electrical anomaly and the magnetic anomaly on the magnetic flux density are different. In the model, taking the line $y = 0$ and drawing the flux density curve as shown in Fig. 8, the start point A and the end point B of the cut line are $(-400, 0)$ and $(400, 0)$, respectively, and the focus of the line and the anomaly are points C and D. When the background environment is air, the presence of anomalous bodies weakens the magnetic flux density, while the magnetic anomalous body is just the opposite case. Since the point A is away from the abnormal body, its magnetic flux density is not affected in the presence nor absence of the abnormal body. The magnetic flux density at the point A can be used as the background environment, that is, the magnetic flux density at the point C in the air. Thus, the degree of change in the magnetic field between the two anomalous bodies is measured by the difference in magnetic flux density between the point A and the point C. It can be seen that the effect of the magnetic anomaly on the magnetic field is 2.5 times that of the electrical anomaly, the ability to change the magnetic field is stronger.

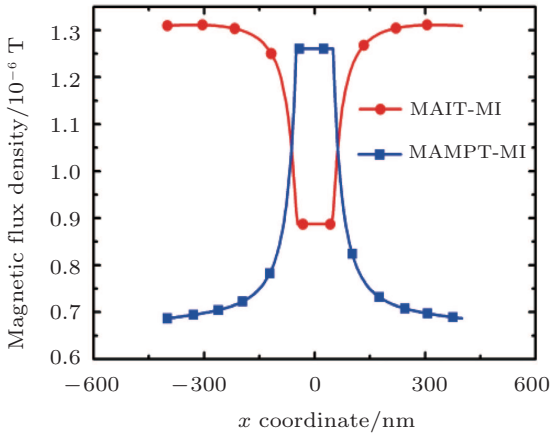


Fig. 8. (color online) The 1D magnetic flux density of MAIT-MI (red line) and MAMPT-MI (blue line).

3.3. Effect of magnetic nanoparticles on sound pressure

The sound sources of the two imaging methods are shown in Eqs. (8) and (11), respectively, to ensure the consistency of the magnetic flux density during the comparative analysis, the sound pressure in the y direction of the MAIT-MI should be compared with the sound pressure in the x direction of the MAMPT-MI . In the simulation model of the two imaging modes, two lines with $x = 0$ and $y = 0$ are taken, and the line intersects the model at four points A, B, C, and D as shown in Fig. 12.

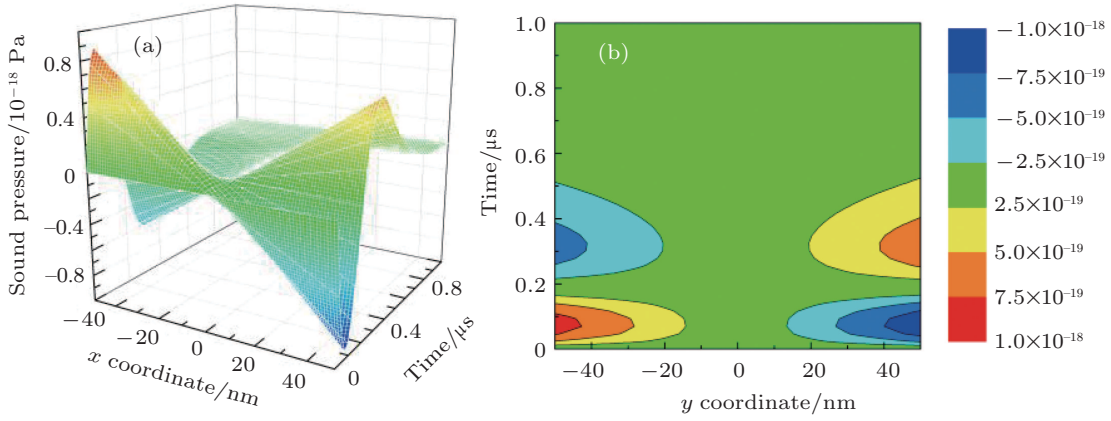


Fig. 9. (color online) MAIT-MI position–time–sound pressure diagrams: (a) the 3D diagram and (b) the 2D color plane diagram.

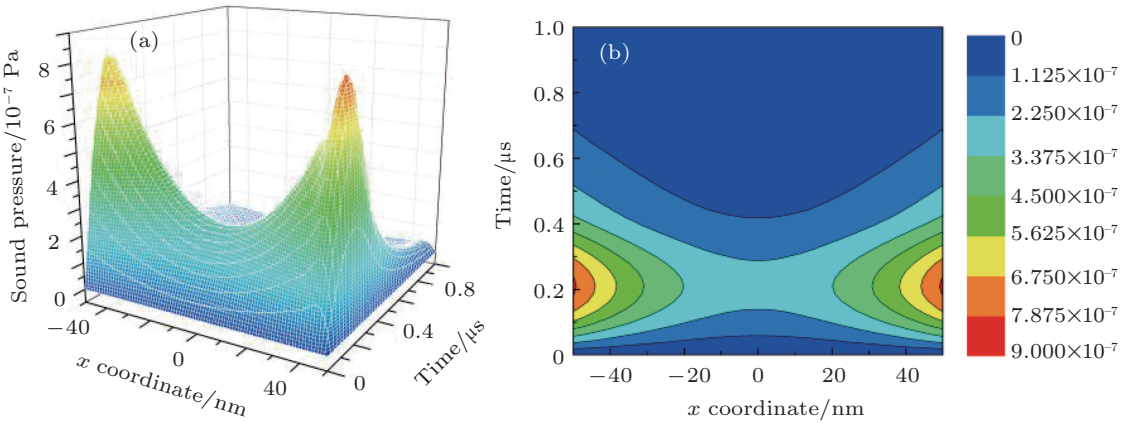


Fig. 10. (color online) MAMPT-MI position–time–sound pressure diagram: (a) the 3D diagram and (b) the 2D color plane diagram.

When comparing the sound pressures, respectively, from the two imaging methods, in order to ensure the reliability of the results, it is necessary to determine the time when the maximum sound pressures from the two method occur. For MAIT-MI and MAMPT-MI, 21 points in a range from −50 nm to 50 nm are scanned in steps of 5 nm on the above two lines, and 101 time points in a range from 0 μs to 1 μs are scanned in steps of 0.01 μs. And calculating the corresponding sound pressure value, the obtained data are drawn into a 3D position-time-sound pressure diagram, and thus obtaining a corresponding 2D color plane diagrams as shown in Figs. 9 and 10. It can be seen from the figure that the sound pressure distribution is symmetrical about the origin of the coordinates. The maximum sound pressure values from the two imaging methods correspond to the time peaks, that is, the maximum sound pressure of MAIT-MI appears at 0.06 μs, and the maximum MAMPT-MI sound pressure occurs at 0.2 μs.

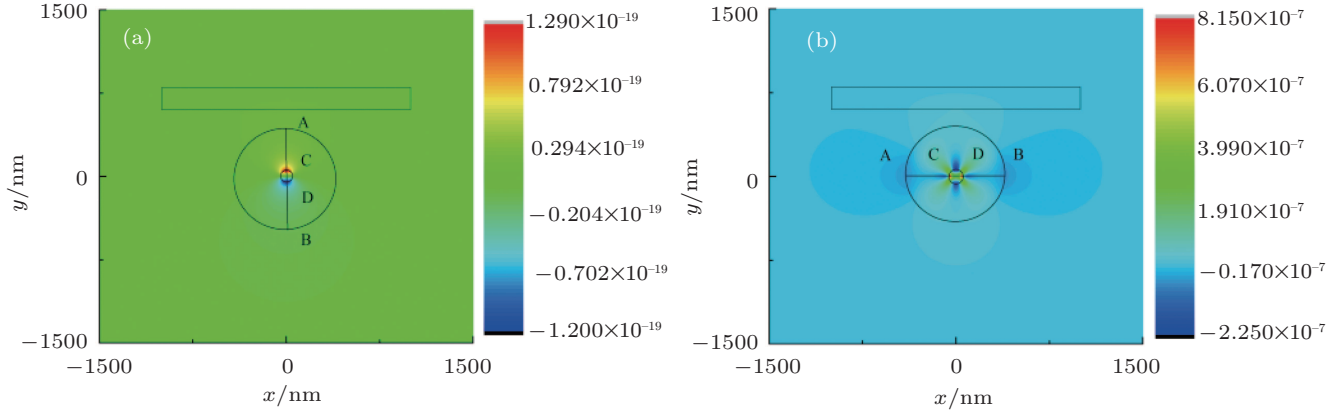


Fig. 11. (color online) Sound pressure distributions of the two imaging methods, obtained according to the peak time calculated by the space-time separation method. (a) $t = 0.06$ μs, MAIT-MI sound pressure; (b) $t = 0.2$ μs, MAMPT-MI sound pressure.

Further, in this article the sound pressure distributions produced by the two imaging methods at their respective peak times are compared as shown in Fig. 11. Since the magnetic nanoparticles are targeted at the diseased tissue, the detection of the magnetic nanoparticles is to detect the boundary of the diseased tissue, and the sound pressure signal generated by the magnetic nanoparticle can reflect the boundary of the diseased tissue. It can be seen that the sound pressure distribution characteristics of the two imaging modes are different, when the sound pressure signal is collected, even if the ultrasonic transducer adopts the ring sweep mode, the weak signals outside the collected sound pressure distribution area cannot be used as effective data for sound source reconstruction, thus leading some of the boundaries of the reconstruction of the sound source to be unclear or even missing. The sound pressure distribution of the MAMPT-MI is relatively uniform, and the signal intensity is 12 orders of magnitude larger than the counterpart of the MAIT-MI, which is convenient for detecting and completing sound source reconstruction.

The 1D graph of the sound pressure is plotted at the taken line, as shown in Fig. 12. In the two curves, abnormal body boundaries can be seen at points C and D, but the sound pressure amplitude of MAMPT-MI is 10^{12} times that of MAIT-MI, the signal is stronger, which is more conducive to sound pressure acquisition.

From the above analyses, the sound pressure signal of

MAIT-MI is obtained when the magnetic field strength is 10^{-6} T. However, in practical applications, the magnetic field of MAT-MI is provided by a static magnetic field with a magnetic field strength in a range from 0.1 T to 1 T. A rough estimate shows that even if the 1T static magnetic field in the MAIT-MI is used to replace the alternating magnetic field, the MAMPT-MI sound pressure signal is 6 orders of magnitude larger than the MAIT-MI. Therefore, it can be preliminarily assumed that the magnetic nano-particles can enhance the signal of MAT-MI and simplify the system.

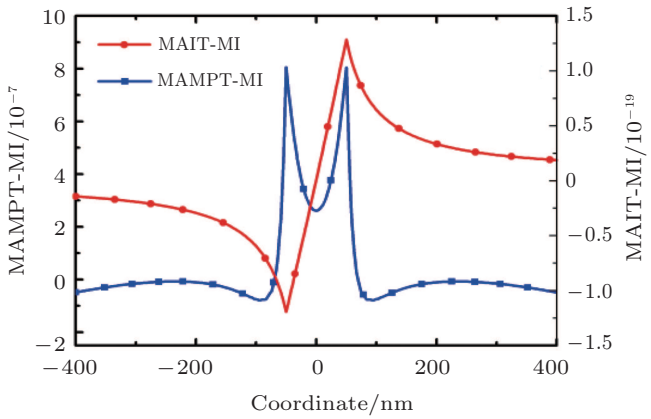


Fig. 12. (color online) The 1D magnetic flux density curves of MAIT-MI (red line) and MAMPT-MI (blue line), respectively.

4. Conclusions and perspectives

In this paper, two imaging methods, i.e., MAIT-MI and MAMPT-MI are simulated by establishing a 2D planar model. Under the same excitation and magnetic field conditions, the source time terms of the two sources are theoretically analyzed and their differences are compared with each other to determine the peak time. Further, the magnetic flux density and the sound pressure are calculated on this basis. Then we obtain the magnetic flux density distribution, magnetic flux density 1D curve diagram and sound pressure distribution, 1D sound pressure curve diagram, 3D sound pressure map, and corresponding 2D color plan. Simulation results are summarized below.

(i) The time peaks calculated by the time-space separation theory under the guidance of the space–time separation theory of the two imaging methods coincide with the time peaks of the sound pressure during the sound pressure analysis. The results show that the time–space separation method is conducive to analyzing the complex sound sources in magneto–acoustic imaging. It also has a guiding effect on the experimental signal acquisition time.

(ii) Under the strict control of variables and the control of precise conditions, the change of the magnetic field is more significant in the magnetic nanoparticle than the changes in the electrical conductivity of the diseased tissue, and then the difference in sound pressure between the two is compared. The results show that the sound pressure signal of MAMPT-MI is larger than that of MAIT-MI, which can significantly increase the sound pressure signal intensity in the absence of static magnetic field. The 1D curve of sound pressure can clearly distinguish where the magnetic nanoparticles are located. The characteristics are obvious, and the enhancement effect of the imaging effect is significant.

The sound pressure distribution of MAMPT-MI is relatively uniform, and the sound pressure signal intensity is greater than that of MAIT-MI. The sound pressure signal is easy to detect during the experiment and the abundant data volume is conducive to the complete and comprehensive sound source reconstruction.

Although the analysis in this paper indicates that the MAMPT-MI can generate larger sound pressure signals and facilitate the detection of diseased tissues from both theoretical and simulation aspect, there are still some shortcomings. There are made some approximations in the theoretical analysis and simulation process, for example, the microstructure of magnetic nanoparticles and the like. Therefore, comparing with MAIT-MI, there is a certain degree of deviation in the amplitude of the magneto-acoustic signal, but it is certain that MAMPT-MI can generate a larger magnetic acoustic signal. The use of magnetic nanoparticles can further achieve the dual purpose of detection and treatment. The MAIT-MI has the advantage of early diagnosis because it does not require magnetic nanoparticles to encapsulate the drug nor bind it to the diseased tissue. Before the tissue changes physiologically, it can detect the change of electrical characteristics. In addition, the establishment and experimental research of 3D models are still needed. The research results may lay the foundation for MAT-MI of magnetically responsive nanoparticle in subsequent experiments and even clinical applications.

References

[1] Xu Y and He B 2005 *Phys. Med. Biol.* **50** 5175
[2] Ma Q Y and He B 2008 *IEEE Trans. Biomed. Eng.* **55** 9748151
[3] Kaytlin B and Bradley J R 2008 *IEEE Trans. Biomed. Eng.* **55** 9921376
[4] Habib A, Simon B and Pierre M 2015 *J. Differ. Equations* **10** 5375
[5] Li X, Xu Y and He B 2007 *IEEE Trans. Biomed. Eng.* **55** 9301459
[6] Xia R M, Li X and He B 2007 *Appl. Phys. Lett.* **91** 083903
[7] Li X, Leo M and He B 2010 *J. Appl. Phys.* **108** 124702
[8] Zhou Y Q Wang J W, Sun X D, Ma Q Y and Zhang D 2016 *J. Appl. Phys.* **119** 094903
[9] Ma Q Y and He B 2007 *Phys. Med. Biol.* **52** 5085
[10] Ma R, Zhou X Q, Zhang S Q, Yin T and Liu Z P 2016 *Phys. Med. Biol.* **61** 8762
[11] Wang J W, Zhou Y Q, Sun X D, Ma Q Y and Zhang D 2016 *IEEE Trans. Biomed. Eng.* **63** 26292332
[12] Marcin Z, Stanislaw G and Adam R Z 2018 *COMPEL* **37** 538
[13] Xia R M, Li X and He B 2009 *IEEE Trans. Biomed. Eng.* **57** 19846363

[14] Habib A, Qiu L Y, Fadil S and Zhan W L 2017 *Inverse Problems* **33** 125006
[15] Leo M, Li X and He B 2010 *IEEE Trans. Biomed. Eng.* **58** 21097372
[16] Leo M, Hu G and He B 2014 *Med. Phys.* **24** 022902
[17] Hu G, Cressman E and He B 2011 *Appl. Phys. Lett.* **98** 023703
[18] Hu G, Li X and He B 2010 *Appl. Phys. Lett.* **97** 103705
[19] Hu G and He B 2012 *Appl. Phys. Lett.* **100** 013704
[20] Carrey J, Connord V and Respaud M 2013 *Appl. Phys. Lett.* **102** 232404
[21] Steinberg I, Ben-David M and Cannot I 2012 *Nanomedicine: Nanotechnology, Biology and Medicine* **8** 569
[22] Fang D W 2014 "Research on magnetoacoustic nano-sensor with magnetic induction", Ph. D. Dissertation (Nanjing: Nanjing Normal University) (in Chinese)
[23] Mariappan L, Shao Q, Yu K, ?et al. 2016 *Nanomedicine: Nanotechnology Biology and Medicine* **12** 689
[24] Liu G Q 2014 Magnetoacoustic tomography technology (Beijing: Science Press) p
[25] Pankhurst Q A, Connolly J and Jones S K 2003 *J. Phys. D: Appl. Phys.* **36** 40035
[26] Wang Z P 2014 "Aggregation of Drug-Loading Particlesin Applied Magnetic Field", Ph. D. Dissertation (Chongqing: Chongqing University) p. 13 (in Chinese)